First-principles calculation of helical spin order in iron perovskite SrFeO₃ and BaFeO₃

Zhi Li,[1,2] Robert Laskowski,[3] Toshiaki Iitaka,[2] and Takami Tohyama[1]

[1]*Yukawa Institute for Theoretical Physics, Kyoto University, Kyoto 606-8502, Japan*
[2]*Computational Astrophysics Laboratory, RIKEN, 2-1 Hirosawa, Wako, Saitama 351-0198, Japan*
[3]*Institute of Materials Chemistry, Vienna University of Technology, Getreidemarkt 9/165-TC, A-1060 Vienna, Austria*

Motivated by the recent discovery of ferromagnetism in cubic perovskite BaFeO₃ under small magnetic field, we investigate spin order in BaFeO₃ and isostructural SrFeO₃ by first-principles calculation. On-site Coulomb and exchange interactions are necessary for the helical spin order consistent with experiments. SrFeO₃ exhibits stable G-type helical order, while A- and G-type helical orders in BaFeO₃ are almost degenerate at a short propagating vector with a tiny energetic barrier with respect to ferromagnetic spin order, explaining ferromagnetism under a small field. The results are consistent with the model calculation in which negative charge-transfer energy is explicitly taken into account.

I. INTRODUCTION

The coexistence of spin order and metallic conductivity in $3d$ transition-metal oxides has attracted a lot of research attention since the discovery of high-temperature superconductivity in copper oxides. The metallic conduction is accessible by the introduction of carriers into either Mott-Hubbard or charge-transfer insulators in the Zaanen-Sawatzky-Allen phase diagram.[1] Without carrier doping, metallic conduction is expected in the phase diagram when systems are located in the area with small or negative charge-transfer energy Δ. Such a situation can be obtained for large atomic number and high valence of $3d$ transition metal.

A typical example of the negative Δ compounds is cubic perovskite SrFeO₃, where the formal valence of iron is Fe^{4+} ($3d^4$) and the effective value of Δ is estimated to be $\Delta \sim -3$ eV.[2] Metallic conductivity has been preserved even below an antiferromagnetic (AFM) transition temperature $T_N \sim 134$ K.[3–5] Below T_N, SrFeO₃ shows a G-type helical spin order whose propagation vector is parallel to the [111] direction. The observed vector is $\mathbf{q} = 0.112(1,1,1) \times 2\pi/a_S$, with lattice parameter $a_S = 3.85$ Å.[6] The magnetic moment is $3.1\mu_B$ per iron at 4.2 K.[7] Recently, a versatile helimagnetic phase diagram under magnetic field was established and unconventional Hall resistivity was discussed in connection with the topological Hall effect in noncoplanar spin texture with scalar spin chirality.[8]

In contrast to SrFeO₃, CaFeO₃ is insulating below 290 K,[9] where a charge disproportionation by the formation of Fe^{3+} and Fe^{5+} emerges.[10] The difference may come from the compression of the lattice due to the small ionic radius of Ca^{2+} compared to Sr^{2+}. It is thus interesting to examine the effect of lattice expansion by replacing Sr^{2+} by Ba^{2+}.

Very recently, cubic BaFeO₃ was synthesized by low-temperature chemistry.[11] The ground state seems to be AFM and there is no charge disproportionation and no structural distortion down to 8 K, similar to SrFeO₃. However, its helical order is different from SrFeO₃: A-type helical order with a propagation vector along the [100] direction. Here, $\mathbf{q} = (0.06,0,0) \times 2\pi/a_B$ with lattice parameter $a_B = 3.97$ Å. By applying small magnetic field ~ 0.3 T, the AFM state changes to a ferromagnetic (FM) one whose saturated moment

is $3.5\mu_B$/Fe. This is also different from SrFeO₃, where saturated ferromagnetism ($3.5\mu_B$/Fe) is achieved by applying more than 40 T.[8]

The helical spin order in iron perovskites has been examined theoretically based on a double-exchange model explicitly including an oxygen $2p$ orbital.[12] By adding superexchange interaction J_{SE} between localized spins, the G-type helical order is stabilized. Although the reduction of J_{SE} changes the G-type to the A-type order in the small and negative Δ region, it is not clear whether the change really corresponds to the difference of real materials between SrFeO₃ and BaFeO₃. In order to include material information in theory, we need to perform a first-principles calculation on magnetic structures in these compounds based on density functional theory (DFT).

In this paper, we perform noncollinear spin polarized DFT calculations in SrFeO₃ and BaFeO₃ as a function of the propagation vector $\mathbf{q}$ for helical spin order. We find that the DFT calculation within the local spin density approximation (LSDA) requires on-site Coulomb interaction U and exchange interaction J to explain experimentally observed propagation vectors. The G-type helical order in SrFeO₃ is nicely reproduced by the LSDA $+$ U with $U = 3$ eV, $J = 0.6$ eV. In BaFeO₃, although the G-type order is lower in energy, the energy difference between A- and G-type orders gets extraordinary small around the experimentally observed propagating vector, in contrast to SrFeO₃. The energy difference between finite $\mathbf{q}$ and $\mathbf{q} = 0$ (FM) orders is larger in SrFeO₃ than in BaFeO₃, which is consistent with the experimental observation that SrFeO₃ requires a larger magnetic field to achieve a saturated FM state. The difference between the two compounds is attributed to the different lattice constants. This is confirmed by performing a model calculation that includes both negative Δ and the difference of the lattice constant through the distance dependence of hopping and superexchange parameters. We also find that the density of states (DOS) just below the Fermi level is dominated by the oxygen $2p$ component, consistent with the view of negative Δ.

This paper is organized as follows. In Sec. II, we introduce the computational method for helical spin order using the DFT. The results by DFT calculation are shown in Sec. III.

In Sec. IV, we introduce a double-exchange model, and we present results consistent with the DFT calculations. We summarize our results from the DFT and model calculations in Sec. V.

II. COMPUTATIONAL METHOD

In order to treat helical spin order, we must constrain the form of the wave function.[13,14] The wave function $\Psi_{\mathbf{k}}(\mathbf{r})$ under the propagation vector $\mathbf{q}$ could be written as

$$\Psi_{\mathbf{k}}(\mathbf{r}) = \begin{pmatrix} e^{i(\mathbf{k}-\mathbf{q}/2)\cdot\mathbf{r}} & 0 \\ 0 & e^{i(\mathbf{k}+\mathbf{q}/2)\cdot\mathbf{r}} \end{pmatrix} \begin{pmatrix} \mu_{\mathbf{k}}^{\uparrow}(\mathbf{r}) \\ \mu_{\mathbf{k}}^{\downarrow}(\mathbf{r}) \end{pmatrix}, \quad (1)$$

where $\mu_{\mathbf{k}}^{\sigma}(\mathbf{r})$ is the translational invariant Bloch wave function with spin σ before transformation. To determine the optimal propagation vector $\mathbf{q}$, we calculate the $\mathbf{q}$-dependent total energy $E(\mathbf{q})$ per unit cell using the VASP code.[15] Noncollinear spin polarized calculations are performed within the LSDA with and without U and J.[16] The calculation is done in a primitive cell with $10 \times 10 \times 10$ k points and an energy resolution 0.01 meV per cell. Since the orbital moment is quenched completely by our calculation, the spin-orbital coupling effect is not under consideration. The cubic crystal structure (space group Pm-$3m$) is used. Crystal distortions may result from the spin lattice coupling, but this distortion is not detected by experiment down to 8 K. We believe, therefore, that the distortion is very small and we ignore it in our calculations.
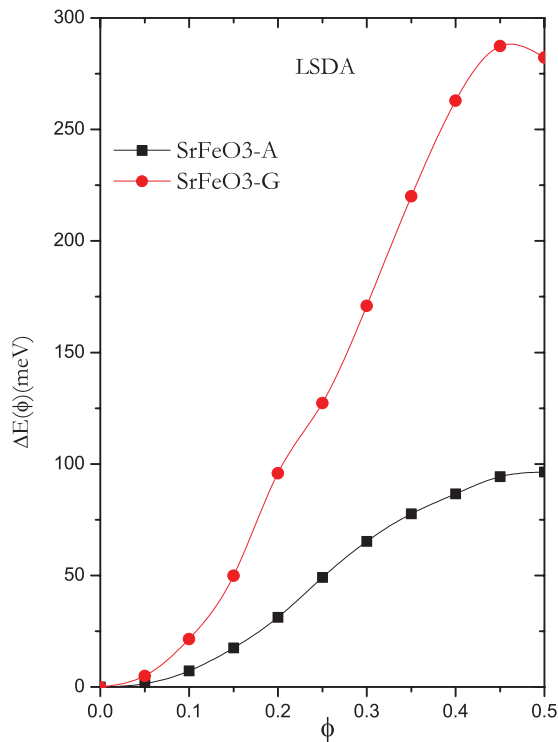
III. RESULTS OF THE DFT CALCULATION

Figure 1 shows the total energy of $SrFeO_3$ as a function of the propagation vector by the LSDA, where ϕ in the horizontal axis is defined by $\mathbf{q} = \phi(1,1,1) \times 2\pi/a_S$ for the G type and $\mathbf{q} = \phi(1,0,0) \times 2\pi/a_S$ for the A type with $a_S = 3.85$ Å.[6] The total energy is measured from the $\phi = 0$ (FM) state: $\Delta E(\phi) \equiv E(\phi) - E(\phi = 0)$. Within the LSDA, the ground state is the FM state. If we take $U = 3$ eV and $J = 0.6$ eV, the minimum energy of $SrFeO_3$ shown in Fig. 2 is located at $\phi = 0.11$, which agrees with the experimental findings. The magnetic field required to overcome the energetic barrier of $\Delta E(\phi = 0.11) = 3.0$ meV is approximately equal to 52 T, which is close to the experimental magnetic field ($\sim$42 T) at which the FM moment is saturated.[8] The calculated moment at $\phi = 0.11$ inside the muffin-tin spheres is $3.0\mu_B$/Fe, close to the experimental value of $3.1\mu_B$/Fe.[7]

$\Delta E(\phi)$ for $BaFeO_3$ with lattice constant[11] $a_B = 3.97$ Å is shown in Fig. 2, where the same U and J are employed. We find that the total energy is almost independent of wave vector in both A- and G-type helical spin orders when $\phi < 0.08$. This is consistent with the fact that the magnetic field needed to obtain the saturated FM state is smaller[11] ($\sim$1 T) than that in $SrFeO_3$. The energy difference between A and G type is tiny, so the A-type helical spin order may be stabilized by, for example, introducing a correlation effect; this is beyond the scope of the present calculation. The small energy difference may affect physical properties at finite temperatures.
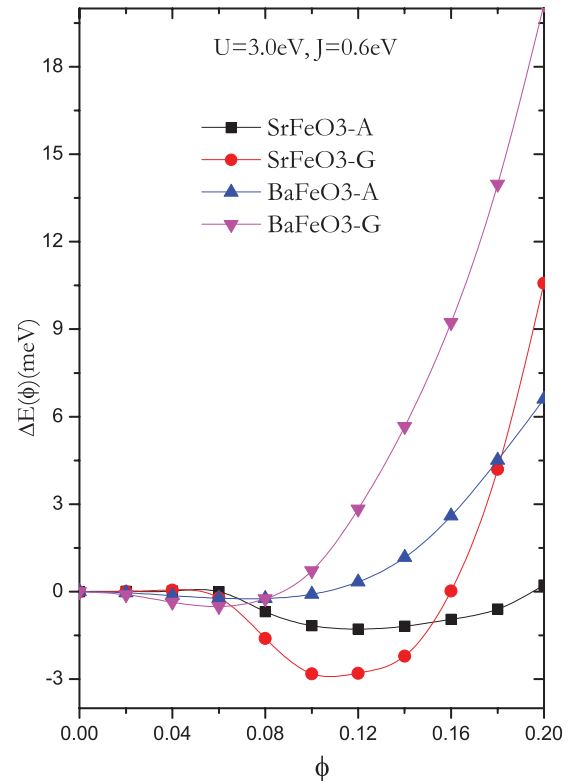

FIG. 1. (Color online) The ϕ dependence of the total energy difference per unit cell, $\Delta E(\phi) \equiv E(\phi) - E(\phi = 0)$, obtained by the LSDA in $SrFeO_3$. For the definition of ϕ, see the text.

FIG. 2. (Color online) The ϕ dependence of the total energy difference per unit cell, $\Delta E(\phi) \equiv E(\phi) - E(\phi = 0)$, obtained by LSDA $+$ U in $SrFeO_3$ and $BaFeO_3$. For the definition of ϕ, see the text.
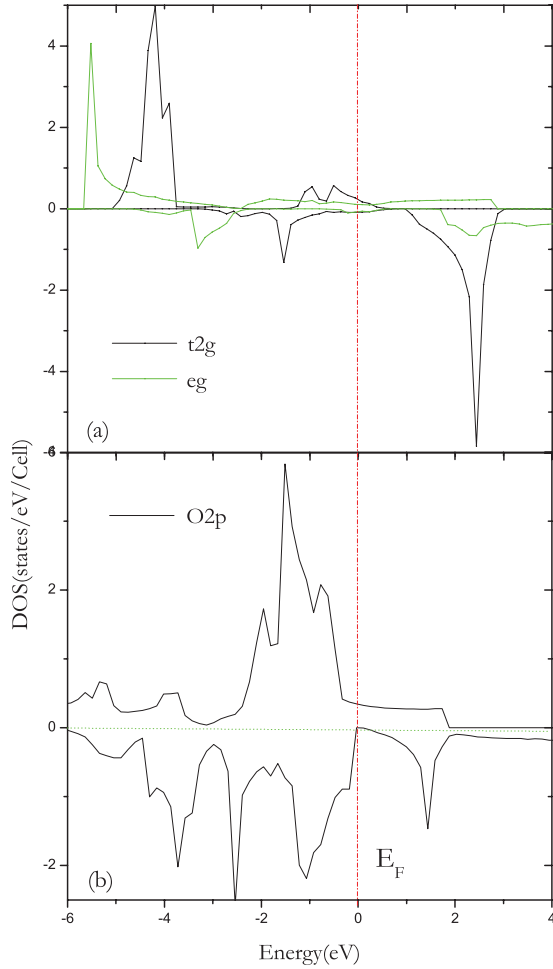
FIG. 3. (Color online) Density of states (DOS) of BaFeO$_3$ in the FM state calculated by LSDA $+$ U with $U = 3.0$ eV and $J = 0.6$ eV. The positive side of the DOS denotes the up-spin DOS, while the negative side denotes the down-spin DOS. Dotted vertical line at zero energy represents the Fermi energy E_F. (a) DOS of Fe $3d$ t_{2g} and e_g orbitals. (b) DOS of O $2p$ orbitals.

In order to clarify the electronic structure of BaFeO$_3$, we show in Fig. 3 the DOS for the FM state ($\phi = 0$), since this state is very close to the stable helical state. Negative DOS represents a down-spin component. The $2p$ electrons of oxygen and $3d$ of iron hybridize intensely in the energy scale -4 to 0 eV, and the spin-up component crosses the Fermi level, which indicates BaFeO$_3$ is half-metallic. The fact that the DOS near the Fermi level is dominated by oxygen $2p$ is consistent with the view of small or negative Δ in high valance $3d$ transition-metal oxides. We also find that the t_{2g} orbitals are almost occupied by up-spin electrons but are empty for down spins. This indicates a localized nature of t_{2g} spins.

What is the origin of different stable helical structures in SrFeO$_3$ and BaFeO$_3$? The most significant effect may come from the lattice parameter based on the results of our DFT calculation. Since the ionic radius of Ba^{2+} is larger than that of Sr^{2+}, BaFeO$_3$ can be considered as expanded SrFeO$_3$. We have confirmed that the energy difference between G type and A type in SrFeO$_3$ decreases upon increasing the lattice parameter (not shown). To get a better understanding of the helical spin

order and the effect of the lattice in SrFeO$_3$ and BaFeO$_3$, we connect our DFT calculation with a double-exchange model in Sec. IV.

IV. RESULTS OF THE MODEL CALCULATION

Mostvoy[12] has shown that a double-exchange model including explicitly oxygen $2p$ orbitals bears the A-type helical spin order of localized t_{2g} spins under small or negative Δ. By adding superexchange interaction J_{SE} between the localized t_{2g} spins, G-type helical order emerges. The Hubbard U in our first-principles calculations is crucial for stabilizing the t_{2g} localized spins so as to be consistent with the double-exchange model. This is realized in Fig. 3, where all of the up-spin electrons of the t_{2g} are deep in energy. In addition, we expect the superexchange process to occur by making use of U, although a precise estimate of the process is difficult. We note that small or negative Δ is necessary for the double-exchange model to produce both the G- and A-type orders. In our LSDA $+$ U calculations, the presence of O $2p$ DOS just below the Fermi level [see Fig. 3(b)] will be indirect evidence of small or negative Δ.

In order to make clear the correspondence between the double-exchange model with J_{SE} and our LSDA $+$ U, we have to show, at least, that the double-exchange model can explain the difference in SrFeO$_3$ and BaFeO$_3$. For this purpose, we examine the model following Mostvoy's procedure.[12] By assuming that the localized t_{2g} spin at site i is in the y-z plane, i.e., $\mathbf{S}_i = S(\hat{\mathbf{y}} \sin \mathbf{q} \cdot \mathbf{x}_i + \hat{\mathbf{z}} \cos \mathbf{q} \cdot \mathbf{x}_i)$ with unit vectors $\hat{\mathbf{y}}$ and $\hat{\mathbf{z}}$ along the y and z directions, respectively, the effective Hamiltonian of the model may be written as[12]

$$H = \sum_{\mathbf{k},\alpha,\delta} t_{\alpha,\delta}(d_{\mathbf{k}\alpha}^{\dagger} P_{\mathbf{k}\delta\downarrow} + \text{H.c.}) + \Delta \sum_{\mathbf{k},\delta,\sigma} P_{\mathbf{k}\delta\sigma}^{\dagger} P_{\mathbf{k}\delta\sigma}$$
$$+ J_{SE} \sum_{\langle i,j \rangle} \mathbf{S}_i \cdot \mathbf{S}_j, \tag{2}$$

with

$$P_{\mathbf{k}\delta\sigma} = 2 \left(\cos \frac{\mathbf{q}_\delta}{4} \cos \frac{\mathbf{k}_\delta}{2} p_{\mathbf{k}\delta\sigma} - \sin \frac{\mathbf{q}_\delta}{4} \sin \frac{\mathbf{k}_\delta}{2} p_{\mathbf{k}\delta-\sigma} \right), \tag{3}$$

where α runs two e_g orbitals of $3z^2 - r^2$ and $x^2 - y^2$, δ runs three components of x, y, and z, $\langle i,j \rangle$ runs the nearest-neighbor pairs, $d_{\mathbf{k}\alpha}$ represents the annihilation of the e_g electron, and $p_{\mathbf{k}\delta\sigma}$ represents the annihilation of the $2p_\delta$ electron with spin σ. The hopping matrix element $t_{\alpha,\delta}$ is given by $t_{3z^2-r^2,x} = t_{3z^2-r^2,y} = -(pd\sigma)/2$, $t_{3z^2-r^2,z} = (pd\sigma)$, $t_{x^2-y^2,x} = -t_{x^2-y^2,y} = \sqrt{3}(pd\sigma)/2$, and $t_{x^2-y^2,z} = 0$, with the hopping parameter $(pd\sigma)$. We ignore oxygen-oxygen hopping for simplicity. We find from (3) that finite $\mathbf{q}$ mixes both down and up spins for holes on oxygen.

We calculate the total energy of the Hamiltonian (2) with one e_g hole[12] and plot it as a function of ϕ for both the G- and A-type helical orders, as shown in Fig. 4. For SrFeO$_3$, we take $\Delta = -3$ eV and $(pd\sigma) = 1.3$ eV according to photoemission analysis.[2] We determine the remaining unknown parameter J_{SE} in order for the energy minimum to be located at the experimentally observed propagation vector, as shown in Fig. 4(a). J_{SE} is then estimated to be $J_{SE} = 9.1$ meV. Using the same parameter set, we find that the minimum energy of
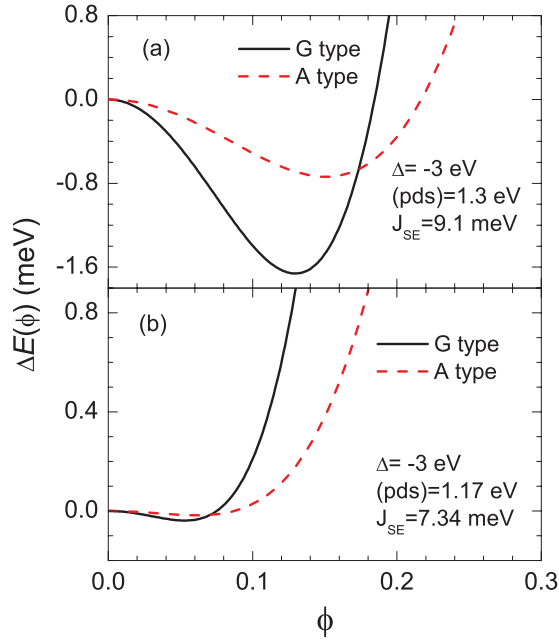
FIG. 4. (Color online) The ϕ dependence of the total energy difference relative to $\phi = 0$, $\Delta E(\phi)$ of model (2). (a) SrFeO$_3$ and (b) BaFeO$_3$. Parameters denoted in each panel are taken so that the minimum of the energy is located at experimentally observed ϕ (see text). The G (A) -type helical spin order is represented by a solid black (broken red) line.

the A-type order is higher by 0.92 meV and the energy of the FM state ($\phi = 0$) is also higher by 1.66 meV. The latter energy corresponds to a magnetic field of 28.7 T, which is slightly smaller than the FM transition field $\sim$42 T for SrFeO$_3$.[8]

For BaFeO$_3$, we use a slightly smaller $(pd\sigma) = 1.17$ eV, taking the lattice expansion into account. By minimizing the energy at around experimentally observed ϕ, we find $J_{SE} = 7.34$ meV, which is smaller than that for SrFeO$_3$ and is a reasonable value as a result of the expansion of the lattice constant compared with SrFeO$_3$. The energy relative to $\phi = 0$ is very small with 0.017 meV, as shown in Fig. 4(b). This value corresponds to 0.3 T, which is comparable to the experimental value of 1 T. Such a small energy difference mainly comes from the decrease of $(pd\sigma)$ as compared with SrFeO$_3$. We note that the reduction of J_{SE} makes the energy difference between the G- and A-type orders considerably small, and the difference becomes almost zero for BaFeO$_3$.

We realize that the results of the model calculation are qualitatively consistent with the LSDA + U results. Quantitative differences may be due to many assumptions for the

construction of the double-exchange model. Nevertheless, the agreement between the model calculation and LSDA + U is satisfactory. This means that the LSDA + U results contain the essential part of the model calculations, i.e., negative Δ and competition between the double-exchange and superexchange processes.

V. SUMMARY

We have examined helical spin order in cubic perovskite SrFeO$_3$ and BaFeO$_3$ by first-principles calculations based on DFT. We have found that U and J are necessary for explaining experimentally observed propagation vectors of spin. Including U and J in the LSDA, we have obtained the G-type helical order for SrFeO$_3$ and almost degenerate A-type and G-type spin order for BaFeO$_3$. The energy difference between the minimum-energy state and the FM state is larger in SrFeO$_3$ than in BaFeO$_3$, which is consistent with the experimental observation that SrFeO$_3$ requires a larger magnetic field to achieve a saturated FM state. The difference between the two compounds is attributed to the different lattice constants. We have shown a clear correspondence between the first-principles calculation based on LSDA + U and the double-exchange model implemented by superexchange interaction, confirming the importance of the competition between double-exchange and superexchange interactions. The correspondence also implies that the characteristics of negative Δ are included in the first-principles calculations. Correspondingly, the DOS of the oxygen $2p$ component in FM BaFeO$_3$ is just below the Fermi level, which is consistent with the view of negative Δ.

[1] J. Zaanen, G. A. Sawatzky, and J. W. Allen, Phys. Rev. Lett. **55**, 418 (1985).

[2] A. E. Bocquet, A. Fujimori, T. Mizokawa, T. Saitoh, H. Namatame, S. Suga, N. Kimizuka, Y. Takeda, and M. Takano, Phys. Rev. B **45**, 1561 (1992).

[3] J. B. MacChesney, R. C. Sherwood, and J. F. Potter, J. Chem. Phys. **43**, 1907 (1965).

[4] T. Takeda, R. Kanno, Y. Kawamoto, M. Takano, S. Kawasaki, T. Kamiyama, and F. Izumi, Solid State Sci. **2**, 673 (2000).

[5] N. Hayashi, T. Terashima, and M. Takamo, J. Mater. Chem. **11**, 2235 (2001).

[6] T. Takeda, Y. Yamaguchi, and H. Watanabe, J. Phys. Soc. Jpn. **33**, 967 (1972).

[7]T. Takeda, S. Komura, and N. Watanabe, in *Ferrites*, edited by H. Watanabe, S. Iida, and M. Sugimoto (Center for Academic Publication, Tokyo, 1981), p. 385.

[8]S. Ishiwata, M. Tokunaga, Y. Kaneko, D. Okuyama, Y. Tokunaga, S. Wakimoto, K. Kakurai, T. Arima, Y. Taguchi, and Y. Tokura, Phys. Rev. B **84**, 054427 (2011).

[9]S. Kawasaki, M. Takano, R. Kanno, T. Takeda, and A. Fujimori, J. Phys. Soc. Jpn. **67**, 1529 (1998).

[10]M. Takano, N. Nakanishi, Y. Takeda, S. Naka, and T. Takeda, Mater. Res. Bull. **12**, 923 (1977).

[11]N. Hayashi, T. Yamamoto, H. Kageyama, M. Nishi, Y. Watanabe, T. Kawakami, Y. Matsushita, A. Fujimori, and M. Takano, Angew. Chem. Int. Ed. **50**, 12547 (2011).

[12]M. Mostovoy, Phys. Rev. Lett. **94**, 137205 (2005).

[13]L. M. Sandratskii, Phys. Status Solidi B **136**, 167 (1986).

[14]R. Laskowski, G. K. H. Madsen, P. Blaha, and K. Schwarz, Phys. Rev. B **69**, 140408(R) (2004).

[15][http://www.vasp.at/].

[16]A. I. Liechtenstein, V. I. Anisimov, and J. Zaanen, Phys. Rev. B **52**, 5467R (1995).